RESEARCH ARTICLE SUMMARY

ORGAN REGENERATION

Reactivation of mammalian regeneration by turning on an evolutionarily disabled genetic switch

Weifeng Lin†, Xiaohui Jia†, Xiaofeng Shi†, Qiuya He†, Panyu Zhang†, Xianglei Zhang, Liping Zhang, Mingqi Wu, Tengfei Ren, Yufei Liu, Haohao Deng, Yanyao Li, Shiqi Liu, Shaoyong Huang, Jingmin Kang, Jun Luo*, Ziqing Deng*, Wei Wang*

Full article and list of author affiliations: https://doi.org/10.1126/science.adp0176

INTRODUCTION: Regeneration, an apparently beneficial trait, is well maintained in some animal lineages but has been lost in many others during evolution and speciation. A complete rescue of organ regeneration in mammals with limited regenerative capacity has not yet been achieved, primarily because of limited information on the linkage between the failure of regeneration and the genetic changes in the genome. Understanding what has occurred during animal evolution to drive the loss or gain of regeneration will shed new light on regenerative medicine.

RATIONALE: Identification of the causal mechanism underlying the failure of regeneration in mammals through comparative strategies is usually entangled by the large phylogenetic distance from highly regenerative species (mostly lower vertebrates). Exploration of principles in the evolution of regeneration demands an organ with easy accessibility and diverse regenerative capacities. One such mammalian organ is the ear pinna, which evolved to funnel sound from the surrounding environment for better distinguishing between ambient noise and predators or prey. The ear pinna possesses complex tissues such as skin and cartilage and exhibits remarkable diversity in the ability to regenerate full-thickness holes punched through this organ in placental mammals.

RESULTS: By performing a side-by-side comparison between regenerative species (rabbits, goats, and African spiny mice) and nonregenerative species (mice and rats), we found that the failure of regeneration in mice and rats was not due to the breakdown of tissue-loss triggered blastema formation and proliferation. Single-cell RNA sequencing and spatial transcriptomic analyses of rabbits and mice identified the response of wound-induced fibroblasts (WIFs) as a key difference between the regenerating and nonregenerating ear pinna. Gene overexpression studies discovered that *Aldehyde Dehydrogenase 1 Family Member A2* (*Aldh1a2*), encoding a rate-limiting enzyme for the synthesis of retinoic acid (RA) from retinaldehyde, was sufficient to rescue mouse ear pinna regeneration. The activation of *Aldh1a2* upon injury was correlated with the regenerative capacity of the tested species. Furthermore, we demonstrated that the deficiency of *Aldh1a2* expression, together with the augmented activity of the RA degradation pathway, contributed to insufficient RA production after injury and eventually the failure of regeneration. An exogenous supplement of RA—but not the synthetic precursor retinol—was sufficient to induce regeneration by directing WIFs to form new ear pinna tissues. The inactivation of multiple *Aldh1a2*-linked regulatory elements accounted for the injury-dependent deficiency of *Aldh1a2* in mice and rats. Importantly, activation of *Aldh1a2* driven by a single rabbit enhancer was sufficient to promote ear pinna regeneration in transgenic mice.

CONCLUSION: Our study identified a direct target involved in the evolution of regeneration and provided a potential framework for dissecting mechanisms underpinning the failure of regeneration in other organs or species. RA signaling is broadly involved in different contexts of regeneration including bone, limb, skin, nerve, and lung regeneration. The crosstalk between the RA pathway and the crucial regeneration regulator, AP-1 complex, further highlights the impact of RA deficiency on regeneration in some lineages. We propose that modulation of the RA pathway may be a hot spot for the evolution of regeneration in vertebrates. □

*Corresponding author. Email: wangwei@nibs.ac.cn (W.W.); dengziqing@genomics.cn (Z.Q.D.); luojun@nwafu.edu.cn (J.L.) †These authors contributed equally to this work. **Cite this article as** W. Lin *et al.*, Science **388**, eadp0176 (2025). DOI: 10.1126/science.adp0176

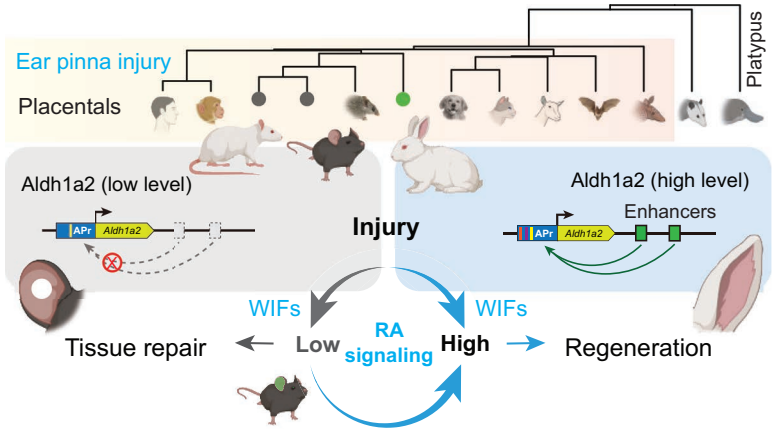

Evolution of regeneration in mammals. In regenerative rabbits, the *Aldh1a2*-linked enhancers interact with the promoter to activate robust expression of *Aldh1a2* upon ear pinna injury. The activities of such enhancers were lost in mice and rats during evolution, resulting in the deficiency of *Aldh1a2* expression and insufficient production of retinoic acid (RA) in these animals. The low RA signaling activities limited the morphogenic potential of WIFs and resulted in failure to regenerate, but switching on *Aldh1a2* or an exogenous supplement of RA was sufficient to reactivate regeneration.

ORGAN REGENERATION

Reactivation of mammalian regeneration by turning on an evolutionarily disabled genetic switch

Weifeng Lin[1,2]†, Xiaohui Jia[1,3]†, Xiaofeng Shi[4]†, Qiuya He[5]†, Panyu Zhang[4]†, Xianglei Zhang[1,2], Liping Zhang[1,2], Mingqi Wu[1,2], Tengfei Ren[1,2], Yufei Liu[1], Haohao Deng[4], Yanyao Li[1,6], Shiqi Liu[1,6], Shaoyong Huang[4], Jingmin Kang[4], Jun Luo[5]*, Ziqing Deng[4]*, Wei Wang[1,2]*

Mammals display prominent diversity in the ability to regenerate damaged ear pinna, but the genetic changes underlying the failure of regeneration remain elusive. We performed comparative single-cell and spatial transcriptomic analyses of rabbits and mice recovering from pinna damage. Insufficient retinoic acid (RA) production, caused by the deficiency of rate-limiting enzyme Aldh1a2 and boosted RA degradation, was responsible for the failure of mouse pinna regeneration. Switching on *Aldh1a2* or RA supplementation reactivated regeneration. Evolutionary inactivation of multiple *Aldh1a2-linked* regulatory elements accounted for the deficient *Aldh1a2* expression upon injury in mice and rats. Furthermore, the activation of *Aldh1a2* by a single rabbit enhancer was sufficient to improve ear pinna regeneration in transgenic mice. Our study identified a genetic switch involved in the evolution of regeneration.

Mammals, including humans, possess limited regenerative capacities for many tissues and organs (*1*, *2*). In humans, traumatic injury to the brain, spinal cord, heart, or limbs leads to impaired or complete loss of organ functions. By contrast, such damage can be fully recovered by regeneration in teleost fish and salamanders (*3*, *4*). Various approaches have been evaluated to stimulate regeneration in nonregenerating organs, including stem cell therapy (*5*–*7*), tissue engineering (*8*), forced expression of proregenerative genes (*9*–*12*), electrical stimulation (*13*, *14*), and neuron transplantation (*15*–*17*). These approaches highlight the possibility of reactivating regeneration in mammals with limited regenerative capacities. However, a complete rescue of organ regeneration has not been achieved, presumably owing to the complexity of mammalian organs, side effects of gene ectopic expression or inhibition, and lack of information on the linkage between the failure of regeneration and the genetic changes in the genome. Understanding what has occurred during evolution to induce the loss or gain of regeneration could provide valuable targets for regenerative medicine.

The identification of causal evolutionary changes associated with regenerative capacities is complicated by the presence of a huge phylogenetic distance between highly regenerative organisms (usually lower vertebrates) and mammals. In theory, a mammalian organ with universality, easy accessibility, and diverse regenerative capacities is suitable for exploring the principles in the evolution of regeneration. One such organ is the ear pinna (the outer ear), a mammal-specific trait that evolved around 160 million years ago to funnel sound from the surrounding environment into the inner ear (*18*). The ear pinna consists of complex tissues, such as skin, cartilage, muscles, peripheral nerves, and blood vessels, and displays prominent diversity in the ability to regenerate full-thickness holes punched through the organ (*19*–*21*). Among the extant mammals, monotremes—including the platypus—lack a visible ear pinna whereas marsupials are incapable of ear pinna regeneration (*22*, *23*). The placentals encompass most mammalian species and exhibit a complex distribution of animals capable and incapable of regeneration in different clades (Fig. 1A). Rabbits, African spiny mice (Acomys), and brush-furred mice are representative animals that can completely restore damage through regeneration (*24*–*26*). Nevertheless, some rodents including mice, rats, guinea pigs, hamsters, and gerbils fail to close punched ear holes (*21*, *22*, *26*, *27*).

Previous studies in rabbits, Acomys, and the super-healing MRL mouse strain suggested that the production of reactive oxygen species, extracellular signal–regulated kinase activities, and myofibroblast fate are altered in nonregenerating mice (*28*–*38*). Loss of function of a cell-cycle regulator p21, inhibition of apoptosis signal-regulated kinase-1, or stabilization of hypoxia-inducible factor 1α can promote ear pinna regeneration in mice (*33*, *34*, *39*). However, the genetic changes responsible for the failure of regeneration during evolution are unknown. Here, we report a comparative study that involves rabbits, goats, Acomys, mice, and rats to characterize the molecular differences between regeneration and tissue repair.

Identification of regeneration-associated genes upon ear pinna injury

Despite the variation in morphology and size, the ear pinnae of different placental mammals possess similar cell types and functions. We compared the regenerative (rabbits, Acomys, and goats) and nonregenerative (mice and rats) species in two major clades (light purple) constituting the majority of placental animals (Fig. 1A and fig. S1). Rabbits could fill the full-thickness holes within 30 days post injury (dpi) and completely restore lost tissues, including the cartilage, at 90 dpi (Fig. 1, B to D). This process requires the formation of a blastema, an injury-induced heterogeneous cell mass that prepares cells to regenerate new tissues (*27*, *40*). By contrast, mice failed to close the holes (Fig. 1, C and D). However, we consistently observed a tiny piece of new cartilage at 90 dpi (Fig. 1D) and no enrichment of collagen deposition at the wounding site compared with the uninjured regions at both early and late stages (Fig. 1E and fig. S2A), implying that extremely weak regeneration occurred in mice.

Similar to rabbits and goats, we detected a blastema-like tissue between 5 and 10 dpi in mice and rats after the completion of reepithelization, as indicated by the presence of Krt14-negative mesenchymal cells above the amputation plane (fig. S2, B to E). Robust cell proliferative response occurred in both regenerating and nonregenerating animals (Fig. 1, F and G, and fig. S3, A to C). Although the percentage of proliferating cells displayed a continuous drop at later stages of injury in rabbits and mice, the latter underwent a much stronger reduction in the mesenchymal region between 10 and 30 dpi (Fig. 1G). In addition, mice exhibited a relatively higher level of apoptosis than rabbits at 30 dpi (fig. S3, D and G). To determine whether the blastema-like tissue is indeed a blastema, we generated transcriptomes for tissues derived from regenerating and nonregenerating animals. Despite the differences in repairing ear pinna damage, the morphology of the newly formed tissues at early stages was comparable across different species when 2-mm ear holes were punched in mice and rats and 4-mm ear holes were punched in rabbits and goats (fig. S2, B to E). Thus,

[1]National Institute of Biological Sciences, Beijing, China. [2]Tsinghua Institute of Multidisciplinary Biomedical Research, Tsinghua University, Beijing, China. [3]College of Biological Sciences, China Agricultural University, Beijing, China. [4]BGI Research, Beijing, China. [5]Shaanxi Key Laboratory of Molecular Biology for Agriculture, College of Animal Science and Technology, Northwest A&F University, Yangling, Shaanxi, China. [6]Graduate School of Peking Union Medical College, Chinese Academy of Medical Sciences, Beijing, China. ***Corresponding author. wangwei@nibs.ac.cn (W.W.); dengziqing@genomics.cn (Z.Q.D.); luojun@nwafu.edu.cn (J.L.)** †These authors contributed equally to this work.

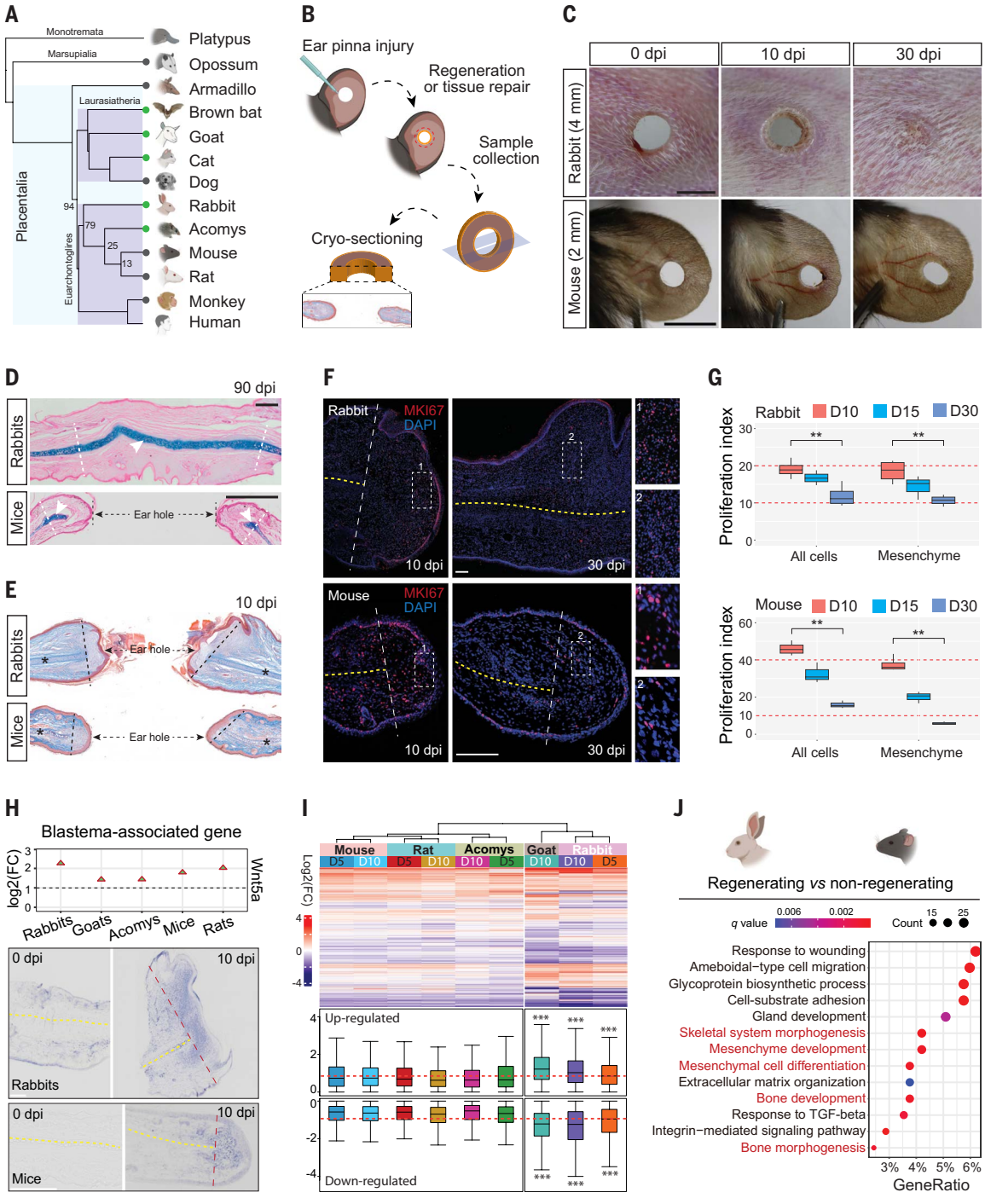

Fig. 1. Evolutionary diversity of injury response upon ear pinna damage in mammals. (**A**) Phylogenetic tree showing the diversity of ear pinna regeneration in mammals. Green and dark gray dots indicate regenerative species and nonregenerative species, respectively. Data are not available for humans. Numbers represent the predicted divergence time (million years ago). (**B**) Scheme of ear pinna injury, sample collection, and cryosection. (**C**) Rabbits could regenerate a 4-mm ear hole within 30 days post injury (dpi) whereas mice failed to close a 2-mm ear hole. Scale bar, 4 mm. $n = 10$ animals. (**D**) Alcian blue staining on rabbit and mouse ear pinna sections at 90 dpi. Arrowheads indicate the new cartilage formed at the amputation site (dashed line). $n = 6$. Scale bar, 500 μm. (**E**) Detection of collagen deposition (blue) using Masson's trichrome staining on rabbit and mouse ear-pinna sections at 10 dpi. Stars indicate cartilage. $n = 6$. (**F**) Cell proliferative response detected by anti-MKI67 (red) antibody at 10 dpi and 30 dpi in rabbits and mice, respectively. The white rectangle highlights the zoomed-in region on each section (right). All images are shown as proximal to the left and distal to the right. The yellow dashed line indicates cartilage. Scale bar, 100 μm. (**G**) The dynamic change of proliferation index at 10 dpi, 15 dpi, and 30 dpi at the wounding site in rabbits and mice. All cells indicate the total number of mesenchymal and epidermal cells above the amputation plane. $^{**}P < 0.01$ (Student's *t*-test). (**H**) Expression of a known blastema-associated gene *Wnt5a* in regenerative species and nonregenerative species at 10 dpi. The in-situ hybridization validated that *Wnt5a* was activated in the blastema in rabbits and mice (bottom). $n = 6$. Scale bar, 250 μm. (**I**) Heatmap showing the expression of one-to-one conserved IRGs in different species. The box plot at the bottom displays the average expression levels for up- and down-regulated genes of each species. $^{***}P < 0.001$ (Wilcoxon tests). (**J**) GO terms enriched for IRGs that were activated in regenerating rabbits but not in nonregenerating mice upon ear pinna damage.

we focused on the 0, 5, and 10 dpi for comparative studies (fig. S4, A and B, and table S1). Combined with the publicly available data from Acomys (*20*), conserved blastema genes including *Wnt5a*, *Fstl1*, and *Tgfb3* (*2*, *41*) were all up-regulated in the tested species regardless of regenerative capacity (Fig. 1H and fig. S4C). For instance, *Wnt5a*, a gene activated in the tail blastema of fish and amphibians, was robustly detected in an equivalent domain at the wounding site in rabbits and mice (Fig. 1H). Thus, the failure of ear pinna regeneration in mice and rats was not due to the breakdown of blastema formation and proliferation at early stages.

To characterize the early injury response among different species, we identified the one-to-one conserved injury-responsive genes (IRGs) that were significantly changed ($\log_2$FC > 0.75 or < −0.75, FDR < 0.05) in at least one tested species (table S2). The clustering analysis showed that the early response in Acomys was closely clustered with mice and rats, but not rabbits and goats. We noted that rabbits and goats activated a relatively stronger response of gene expression (both up- and down-regulated) than the other three species (Fig. 1I). Because only a small percentage of IRGs were commonly activated in the three regenerative species, it is challenging to understand what biological processes were altered in nonregenerative species using multiple-species analyses. To overcome this issue, we compared the IRGs activated in mice or rats with those in rabbits to identify differential IRGs that were only present during regeneration. Taking the mouse-rabbit comparison as an example, the analysis uncovered 469 rabbit-enriched IRGs that were missing in mice (table S2). We define the IRGs only triggered during regeneration as regeneration-associated genes (RAGs). Gene ontology (GO) analysis showed that the representative GO terms enriched for the RAGs were "skeletal system morphogenesis" and "mesenchyme development" (Fig. 1J and fig. S4, D to E). Thus, ear pinna damage in nonregenerative animals successfully activated IRGs essential for blastema formation and proliferation but insufficiently activated RAGs involved in tissue morphogenesis.

Wound-induced fibroblasts are the primary cell source for the expression of RAGs

To investigate the cell response upon injury and determine what cells mainly deploy the RAGs, we carried out single-cell RNA-seq (scRNA-seq) at 0, 5, and 10 dpi in rabbits and mice. Unsupervised analyses unveiled 21 clusters from 32,557 cells in rabbits (Fig. 2A and fig. S5) and 26 clusters from 32,469 cells in mice (Fig. 2B and fig. S6). An integrated analysis of the two datasets confirmed the shared major cell types including keratinocytes, fibroblasts, muscle cells, chondrocytes, and macrophages (fig. S7A). Next, we analyzed the RAGs and found that they were mainly expressed in a subpopulation of fibroblasts that appeared only after tissue damage (Fig. 2C). These wound-induced fibroblasts (WIFs) were present in both species (fig. S5D and S6D). An independent clustering of all fibroblasts unveiled 10 subpopulations (RF0-9) in rabbits and 6 subpopulations (MF0-5) in mice (Fig. 2D and fig. S7). The WIFs could be marked and validated by the expression of *Cr2* (RF1) in rabbits and by *Tnn* (MF3) in mice (Fig. 2, E to G). Furthermore, the RNA velocity analysis showed a distinct direction of cell transitions (arrows) for the WIFs in rabbits and mice at 10 dpi (Fig. 2H), indicating a differential response of WIFs between regeneration and tissue repair.

A side-by-side comparison identified 114 genes that were robustly activated in rabbit WIFs but barely detectable in mouse WIFs (table S3). This cohort of genes includes multiple known morphogenetic factors (*Lef1*, *Bmp2*, *Fgf18*, *Scube2*, and *Pdgfd*) that have been previously suggested to regulate many aspects of development and regeneration (Fig. 2I and fig. S7H) (*42*–*46*). Conversely, we observed increased expression of the myofibroblast marker *Acta2* (also known as α-*SMA*) in mouse WIFs (Fig. 2I and fig. S7H). The top GO terms enriched for these 114 genes were bone development–related biological processes (fig. S7I), which was consistent with the analysis of RAGs (Fig. 1J). In addition to genes linked to the known pathways involved in ear pinna regeneration, we identified many potential regulators with unknown functions, such as *Fads3*, *Nes*, *Sncaip*, *St3gal5*, and *Znf827* (fig. S7J). In sum, our data suggested that WIFs were the primary cell type that deployed the RAGs during regeneration and highlighted the differential molecular response between regenerating and nonregenerating WIFs.

The microenvironment of WIFs is altered in tissue repair

To validate the molecular differences between the two distinct types of WIFs and investigate the spatial response of the scRNA-seq-identified cell populations, we performed spatially resolved transcriptomic analyses using Stereo-seq in rabbits and mice. Cryosections with 10-μm thickness that approximately contained a single-cell layer of ear pinna tissue were collected for analysis at 0, 5, and 10 dpi (fig. S8 to S10). Using the Louvain algorithm, we obtained eight and seven major cell clusters that spatially mapped onto the DAPI-stained anatomical regions of each sequenced section for rabbits and mice, respectively (Fig. 3, A and B). By combining the unsupervised clustering analysis based exclusively on gene expression and marker genes established by scRNA-seq, we determined the primary cell types (keratinocytes, fibroblasts, chondrocytes, muscle cells, and immune cells) and annotated the subclusters of fibroblasts (Fig. 3, A and B). The spatial distribution of signals was further validated through the known marker genes including *Wnt5a*, *Krt5*, *Cr2*, and *Tnn* (Fig. 3C and figs. S9E and S10E). In line with the *Cr2* and *Tnn* expression (Fig. 2G), WIFs were mapped into the blastemal region at the distal mesenchyme for both species (Fig. 3, A and B). Considering that the blastema is defined as maintaining the highest developmental potential in a regenerating organ, we performed CytoTRACE analyses to validate the data further (*47*). As expected, less-differentiated cells with high CytoTRACE scores (red) were localized in the blastema, indicating relatively high quality of our Stereo-seq data (Fig. 3D). Using the chondrocytes of each species as an internal control, the significant difference ($P < 0.001$) between the two normalized scores suggested that rabbit blastema tended to have a relatively higher developmental potential than the mouse blastema (Fig. 3D), which was consistent with the deficiency of critical morphogenetic factors in mice (Fig. 2I).

Efficient regenerative outgrowth is intricately linked with cross-talk among blastema cells, neighboring cells, and the extracellular matrix (ECM). The regenerating blastema cells control their own proliferation and differentiation by communicating with neighboring cells, including epidermal cells, immune cells, and other cell types within the microenvironment. To understand the major differences in blastema microenvironment between mice and rabbits, we first examined the expression of ECM genes. The results revealed significant ($P < 0.001$) alterations of multiple known regeneration-related ECM genes including *Mmp9* (*48*), *Mmp13* (*49*), *Efemp1* (*50*), and *Col15a1* (*51*) in mice (fig. S11, A and B). Furthermore, we carried out ligand-to-target signaling analyses between the WIFs (receiver) and neighboring cells (senders) at 10 dpi using the NicheNet program (*52*). In rabbits, we found that the top ligands exerting robust activities on the WIFs were *Npnt* from keratinocytes and *Bmp2* and *Bmp5* from the muscle cells (fig. S11C). These three genes are known regulators of bone morphogenesis (*44*, *53*, *54*). By contrast, the top ligands received by the mouse WIFs were Il1b and Tnf from the neutrophils. As a result, a different set of predicted target genes was activated in mouse WIFs compared with rabbit WIFs (fig. S11C), suggesting that mice activated an altered microenvironment for WIFs.

Next, we sought to identify the potential major effectors responsible for the failure of regeneration in mice. The Stereo-seq data validated 56 genes with major changes in the spatial pattern between rabbit and mouse WIFs (table S3). For example, the expression of *Scube2* and *Srfbp1* was robustly detected in rabbit WIFs but barely detectable in mouse WIFs (Fig. 3E). Increasing evidence suggests

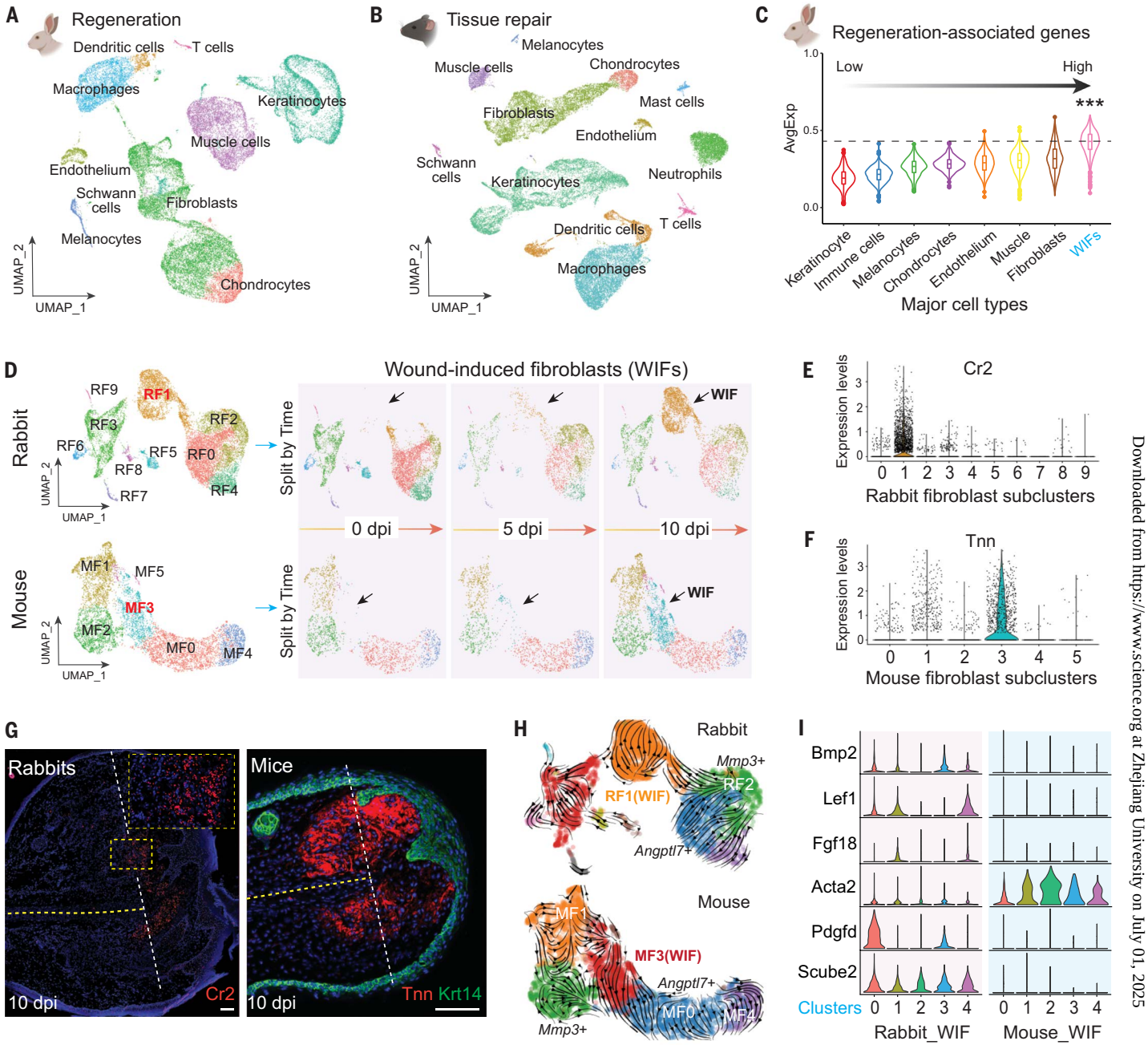

Fig. 2. Single-cell analyses identified differential cell response of wound-induced fibroblasts between rabbits and mice. (**A** and **B**) Uniform manifold approximation and projection (UMAP) plot showing the major cell populations identified at 0 dpi, 5 dpi, and 10 dpi during rabbit ear pinna regeneration (A) and mouse tissue repair (B). 32, 557 and 32,469 cells were analyzed for rabbits and mice, respectively. (**C**) The expression of 469 regeneration-associated genes was mainly enriched in WIFs. ***$P < 0.001$ (Wilcoxon tests). (**D**) Reclustering of fibroblasts detected in scRNA-seq identified 10 subclusters (RF0 to RF9) in rabbits and 6 subclusters (MF0 to MF5) in mice. The split time point for the fibroblasts is shown on the right. RF1 and MF3 are WIFs in rabbits and mice, respectively. (**E** and **F**) Violin plots showing the expression of the marker gene for rabbit WIFs (*Cr2*) and mouse WIFs (*Tnn*). (**G**) The expression of *Cr2* (RNAscope) and *Tnn* (anti-Tnn antibody) at 10 dpi in rabbit and mouse ear pinna, respectively. Krt14 labels the epithelial cells (right). The amputation plane is indicated by the white dashed line. Scale bar, 100 μm. (**H**) RNA velocity analyses showing differential cell response of WIFs between rabbits and mice upon injury. Arrows indicate the predicted direction of cell transitions. (**I**) Violin plots showing the differential expression of *Bmp2*, *Lef1*, *Fgf18*, *Acta2* (α-*SMA*), *Pdgfd*, and *Scube2* between rabbit and mouse WIFs. All subclusters of WIFs were used for the analysis.

that regeneration in different systems and organisms repeatedly deploys conserved genes and signaling pathways involved in fundamental processes such as proliferation and morphogenesis (*55*). To identify commonly activated genes in animals with high regenerative potential, the 56 genes were examined in previously published scRNA-seq datasets for zebrafish caudal fin regeneration and axolotl limb regeneration (*2*, *56*). The majority of the genes were only detected in one type of blastema, because of either species specificity or the sensitivity of scRNA-seq. Notably, we found that activation of nine genes, including *Wnt11*, *St3gal5*, *Srfbp1*, *Sncaip*, *Pdgfd*, *Mmp13*, *Epha7*, *Plcl2*, and *Aldh1a2*, was commonly observed in the highly regenerative blastema, implying potential pivotal roles of these genes

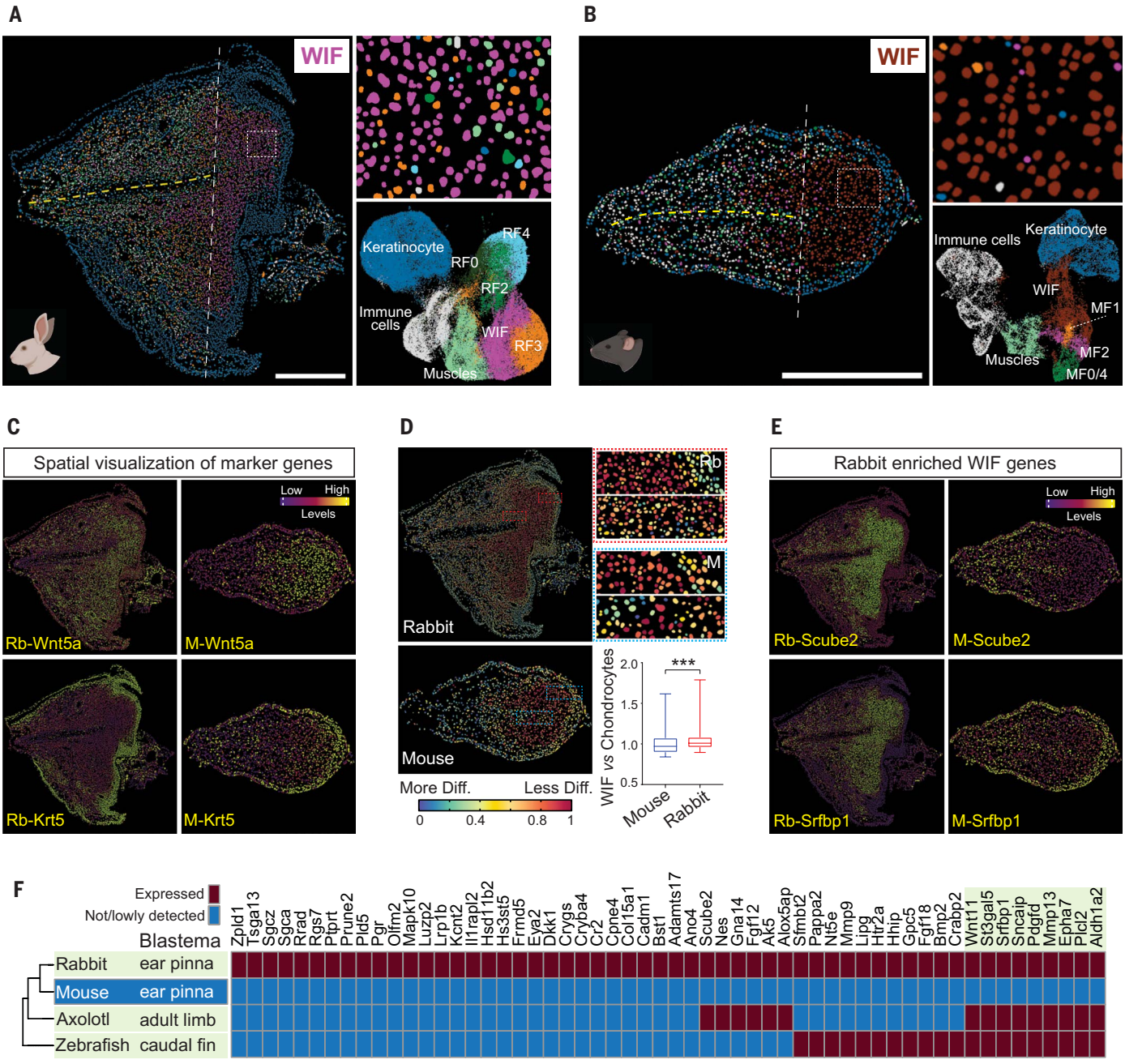

Fig. 3. Comparative spatial transcriptomic atlases of ear pinna regeneration and repair. (**A** and **B**) Stereo-seq enables spatially resolved transcriptomics with high definition in the regenerating rabbit ear pinna (A) and the nonregenerating mouse ear pinna (B). Stereo-seq– identified cell populations (bottom right) were mapped on a DAPI-stained ear pinna section with clear anatomical regions (left). Yellow and white dashed lines indicate the cartilage and the amputation site, respectively. The rectangle highlights a zoomed-in region (top right) in the blastema. The subclusters of fibroblasts are named according to the scRNA-seq data. The same color was used to mark the same cell cluster in each graph. Scale bar, 500 μm. (**C**) Spatial visualization of the expression of a conserved blastema-associated gene *Wnt5a* and an epithelial marker *Krt5* in rabbits (left) and mice (right). Rb, rabbits; M, mice. (**D**) CytoTRACE analysis showing the spatial distribution of the cell differentiation states on rabbit and mouse ear pinna sections. The rectangles (top left) highlight the zoomed-in regions (right). The relative CytoTRACE scores (bottom right) for the WIFs were obtained by normalizing the score of WIFs to that of chondrocytes in each species. ***$P < 0.001$ (Student's *t*-test). (**E**) Spatial visualization of two representative Stereo-seq-validated genes. These genes were robustly detected in rabbit WIFs but not mouse WIFs. (**F**) Identification of commonly activated genes in the blastema of animals with high regenerative potential. Red, the gene is activated based on scRNA-seq data. Blue, the gene is not or lowly detected. Nine genes correlated with the regenerative potential are highlighted in light green (top right).

during regeneration (Fig. 3F and fig. S12). Collectively, the spatial transcriptomics data combined with scRNA-seq data revealed an altered microenvironment for WIFs activated during tissue repair and identified the candidates of potential effectors determining regeneration versus tissue repair.

Insufficient production of retinoic acid is a causative mechanism for the failure of ear pinna regeneration

To determine the functional significance of the potential effectors in the failure of regeneration, we conducted adeno-associated virus (AAV)-based gene overexpression studies during mouse ear pinna

injury. A comparison of 14 different AAV serotypes revealed that AAV7, AAV8, AAV9, and AAV PHP.S were suitable for delivering genes of interest to the mesenchyme of uninjured ear pinna (fig. S13, A to E). However, regular AAVs failed to deliver stable expression of target genes in the rapidly proliferating mesenchyme after injury (fig. S13F). To address this problem, we used a transposase-mediated somatic integration for obtaining stable expression (fig. S13G and Fig. 4A). With this system, we identified two genes that could significantly promote mouse ear pinna regeneration (fig. S14A-B; FDR < 0.001): *Serum Response Factor Binding Protein 1* (*Srfbp1*) and *Aldehyde Dehydrogenase 1 Family Member A2* (*Aldh1a2*). Transcriptomic analysis showed that the functional effect of *Srfbp1* may be related to the enhanced expression of *Fgf9* and *Inhba* (fig. S14C), two known factors involved in regeneration (*2*, *57*, *58*). Unlike the partial rescue of regeneration for *Srfbp1*, the gene *Aldh1a2*, encoding a rate-limiting enzyme in the synthesis of retinoic acid (RA) from retinaldehyde, was sufficient to fully restore ear pinna regeneration (Fig. 4B and fig. S14D). The cellular level of RA is tightly regulated through the balance between its production by synthesizing enzymes (Aldh1a1, Aldh1a2, and Aldh1a3) and degradation by the cytochrome P450 enzymes (Cyp26a1, Cyp26b1, and Cyp26c1) in vertebrates (*59*). The expression of *Aldh1a2* in rabbits was robustly activated after injury and maintained throughout regeneration, with higher expression in the mesenchyme than in the epidermis (Fig. 4C and fig. S14, E to H). By contrast, *Aldh1a2* expression was barely detectable throughout tissue repair in mice (Fig. 4D and fig. S14I). Similarly, we observed significant up-regulation of *Aldh1a2* in other regenerative species and significant down-regulation in nonregenerating rats (Fig. 4D). In terms of the degradation enzymes, we performed RNAscope in situ hybridization analysis for *Cyp26a1* and *Cyp26b1* because *Cyp26c1* was not expressed in the ear pinna of both species according to the RNA-seq data. Indeed, *Cyp26a1* was activated at the wounding site in mouse ear pinna but barely detectable in rabbits whereas *Cyp26b1* was detected in both species with expression mainly enriched in the lateral mesenchyme (fig. S14, J and K). Thus, the synthetic pathway for RA was suppressed and the degradation pathway boosted during injury in mice.

Given that the strong correlation between *Aldh1a2* activation and regenerative capacity, the ability to fully rescue regeneration and the known function of the RA pathway in the regulation of organ development and regeneration in various systems (*60*–*64*), we propose that insufficient production of RA is responsible for the failure of ear pinna regeneration during evolution. If true, supplementation of exogenous RA should be sufficient to reactivate regeneration. Thus, we conducted a series of intraperitoneal injections of RA, retinol (the synthetic precursor of RA), talarozole (TLZ, a Cyp26 inhibitor), and DMSO (control) in mice using a dosage without visible side effects (fig. S15, A and B). As predicted, animals with the exogenous delivery of RA (FDR < 0.001) but not retinol and TLZ fully regenerated the ear holes at 30 dpi (Fig. 4, E to F). Our results differed from the observation of previous studies, in which only coadministration of RA and zebularine (a DNA methyltransferase inhibitor) nearly closed the ear hole whereas RA or zebularine alone could not (*30*, *32*). Such discrepancy is likely due to the short elimination half-life of RA in vivo (*65*), with continuous supplementation of RA required for maintaining its biological activities. The insufficiency of retinol and TLZ in rescuing regeneration confirmed that the RA synthetic pathway was suppressed upon tissue damage in mice. In addition, coinjection of RA and TLZ accelerated regeneration compared with RA alone, indicating that the degradation pathway contributed to final RA levels during tissue repair (Fig. 4F and fig. S15A). Activation of RA signaling allowed regeneration of both the missing structures such as cartilage and nerves, compared with the control (Fig. 4, G to H). To understand when RA signaling activities were required after injury, we performed RA injections at three major stages: blastema formation (0 to 8 dpi, early), blastemal outgrowth (6 to 16 dpi, middle), and tissue morphogenesis (16 to 30 dpi, late). Activation of the RA pathway promoted regeneration at all tested stages, with a stronger effect during blastema formation and outgrowth (FDR < 0.001, Fig. 4I). Next, we asked whether RA signaling was sufficient to rescue rat regeneration and essential for rabbit regeneration. Similar to mice, intraperitoneal injection of RA completely restored the ear holes at 30 dpi in rats (Fig. 4J, $P < 0.001$). Conversely, inhibition of RA synthesis impaired the closure of ear holes in rabbits by treating animals with diethylaminobenzaldehyde (DEAB, Fig. 4K and fig. S15, C and D; $P < 0.001$), a potent inhibitor of RA synthesizing enzymes (*66*). Thus, insufficient production of RA, prompted by the deficiency of a rate-limiting enzyme Aldh1a2 and the enhanced degradation pathway, was responsible for the failure of ear pinna regeneration in mice.

Reactivation of RA signaling triggers a rabbit-like regeneration response that directs WIFs to form new ear pinna tissues

Because WIFs are the cell population with the highest developmental potential, we asked whether they were the cell source for ear pinna regeneration. In the wild-type (WT) mice, the WIF marker gene *Tnn* was barely detectable in intact ear pinna but robustly activated upon injury (Fig. 5A and fig. S16A). Nevertheless, the *Tnn* expression domain regressed at later stages of tissue repair and was restricted to a small region above the stump of the cartilage, resulting in *Tnn*-negative cells dominating the original blastemal region at 30 dpi (Fig. 5B). To determine the lineage commitment of the WIFs by the end of tissue repair, we generated the *Tnn-P2A-Cre-ERT2* mice by inserting the *Cre-ERT2* cassette into the endogenous *Tnn* locus (fig. S16, B and C). We then crossed *Tnn-P2A-Cre-ERT2* with *Ai14* (*Rosa-CAG-LSL-tdTomato*) mice to conduct lineage tracing analyses (fig. S16, D and E). Intraperitoneal injection of tamoxifen in *Tnn-P2A-Cre-ERT2;Ai14* mice before injury failed to activate the expression of tdTomato (fig. S16F). By contrast, the whole mesenchyme above the amputation plane expressed tdTomato at 30 dpi when tamoxifen was injected after injury (fig. S16F). Thus, the original WIFs did not disappear but rather lost *Tnn* expression. We repeated the same experiment in RA-treated animals in which regeneration was fully restored. As a result, all the regenerated mesenchymal tissues were tdTomato-positive, denoting that they were derived from the WIFs (Fig. 5C). Furthermore, we examined which resident cells present during homeostasis contributed to the WIFs. With the hypothesis of cartilage contribution, the lineage tracing analysis using *Acan-CreERT2;Ai14* uncovered that *Acan*+ chondrocytes were a crucial source for WIFs, although not the only one (fig. S16G).

To investigate the mechanisms underlying RA-dependent regeneration, we conducted scRNA-seq on RA-treated and DMSO-treated (control) animals at 15 dpi, the point at which the two groups started to differ in ear hole size. Unsupervised analyses of 26,764 cells derived from the control and 28,753 cells from RA-treated mice uncovered all major cell types identified at early stages (Fig. 5, D and E, and Fig. 2B). As expected, RA treatment significantly promoted the expression of RA receptors (*Rara* and *Rarg*) and RA-responsive genes (*Rai14* and *Rbp1*) in WIFs and other cell clusters (fig. S16H). The activation of RA signaling neither induced a new cell population nor eliminated an existing population (Fig. 5D and fig. S16I). However, RNA velocity analysis of all mesenchymal cells implied that there was an enhanced cell state transition from WIFs and *Mmp3*+ cells (cluster 4) to *Angptl7*+ cells (cluster 3) and a transition from *Mmp3*+ cells to *Coch*+ cells (cluster 6) in RA-treated animals (Fig. 5F). The large interspecies difference makes it challenging to directly compare the similarity between rabbit regeneration and RA-induced regeneration using correlation analysis or principal component analysis. However, RA-induced mouse regeneration promoted the expression of many (40 out of 114) rabbit-enriched WIF genes in mouse WIFs including *Bmp2* (fig. S17A), a crucial factor required for chondrocyte

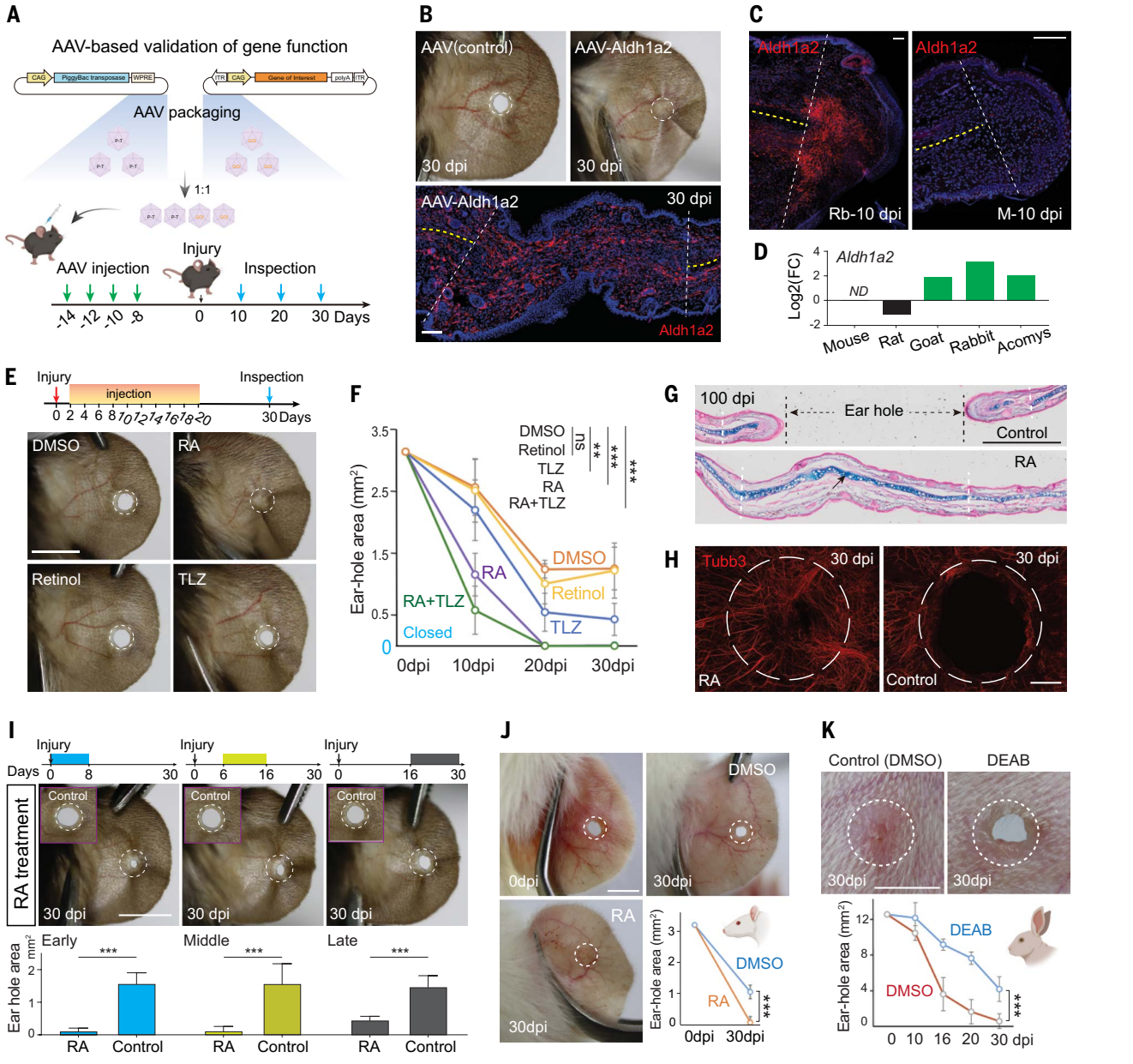

Fig. 4. Deficient *Aldh1a2* expression causes the failure of mouse ear pinna regeneration. (**A**) The strategy for the AAV-based stable gene activation in ear pinna through transposase-mediated somatic integration. (**B**) Overexpression of *Aldh1a2* in mice fully restored the ear pinna regeneration compared with the control at 30 dpi. $n = 10$ (animals). (Bottom) Validation of Aldh1a2 overexpression through anti-Aldh1a2 antibody. Scale bar, 100 μm. (**C**) Aldh1a2 was strongly activated at 10 dpi in rabbit ear pinna (left) but barely detected in mouse ear pinna (right). $n = 6$. Scale bar, 100 μm. (**D**) *Aldh1a2* was significantly up-regulated in regenerating ear pinna but down-regulated or barely detected in nonregenerating ear pinna. Bulk RNA-seq data were used. (**E**) Intraperitoneal injection of retinoic acid but not retinol, TLZ, and DMSO fully restored ear pinna regeneration in mice. Injection of TLZ reduced the size of ear holes but failed to close them. (Top) Injection strategy. $n = 10$. (**F**) Quantification of the ear-hole area in animals subjected to intraperitoneal injections. ns, not significant. **FDR < 0.01. ***FDR < 0.001. (**G**) Activation of RA signaling completely restored the missing cartilage (arrow) at 100 dpi compared with the control (top). Scale bar, 500 μm. (**H**) Reinnervation (left) was detected using the anti-beta III Tubulin antibody at 30 dpi in RA-treated animals. Scale bar, 500 μm. (**I**) The effect of RA on the early, middle, and late stages of ear pinna injury. (Top) Time window for injection. $n = 6$. ***FDR < 0.001. (**J**) Intraperitoneal injection of retinoic acid completely rescued rat ear pinna regeneration. $n = 6$. ***$P < 0.001$ (Student's *t*-test). (**K**) Inhibition of RA synthesizing enzymes with DEAB impaired ear pinna regeneration in rabbits. $n = 6$. ***FDR < 0.001. Student's *t*-test and Benjamini-Hochberg procedure were performed for (F), (I), and (K). Scale bar (E), (I), (J), and (K), 4 mm. The dashed circle labels the amputation site.

proliferation and differentiation. Activation of *Bmp2* using AAV reduced the ear hole size in mice (Fig. 5G and fig. S17, B and C). As seen in rabbits, we observed a significant reduction in the expression of myofibroblasts marker *Acta2* in RA-treated mice (Fig. 5H, Fig. 2I, and fig. S7H). We also found the expression of *Keratin-17*—a gene with sustained activation in regenerating epidermis wounds in rabbits (fig. S17D) and in African spiny mice but not nonregenerating mice (*25*)—was significantly ($P < 0.01$) boosted in RA-treated animals (fig. S17E). Furthermore, we examined the average expression of a collection of known RA-responsive genes (table S3) to understand the strength of the RA response upon injury. Among different clusters, WIFs displayed the most robust RA response in both rabbits

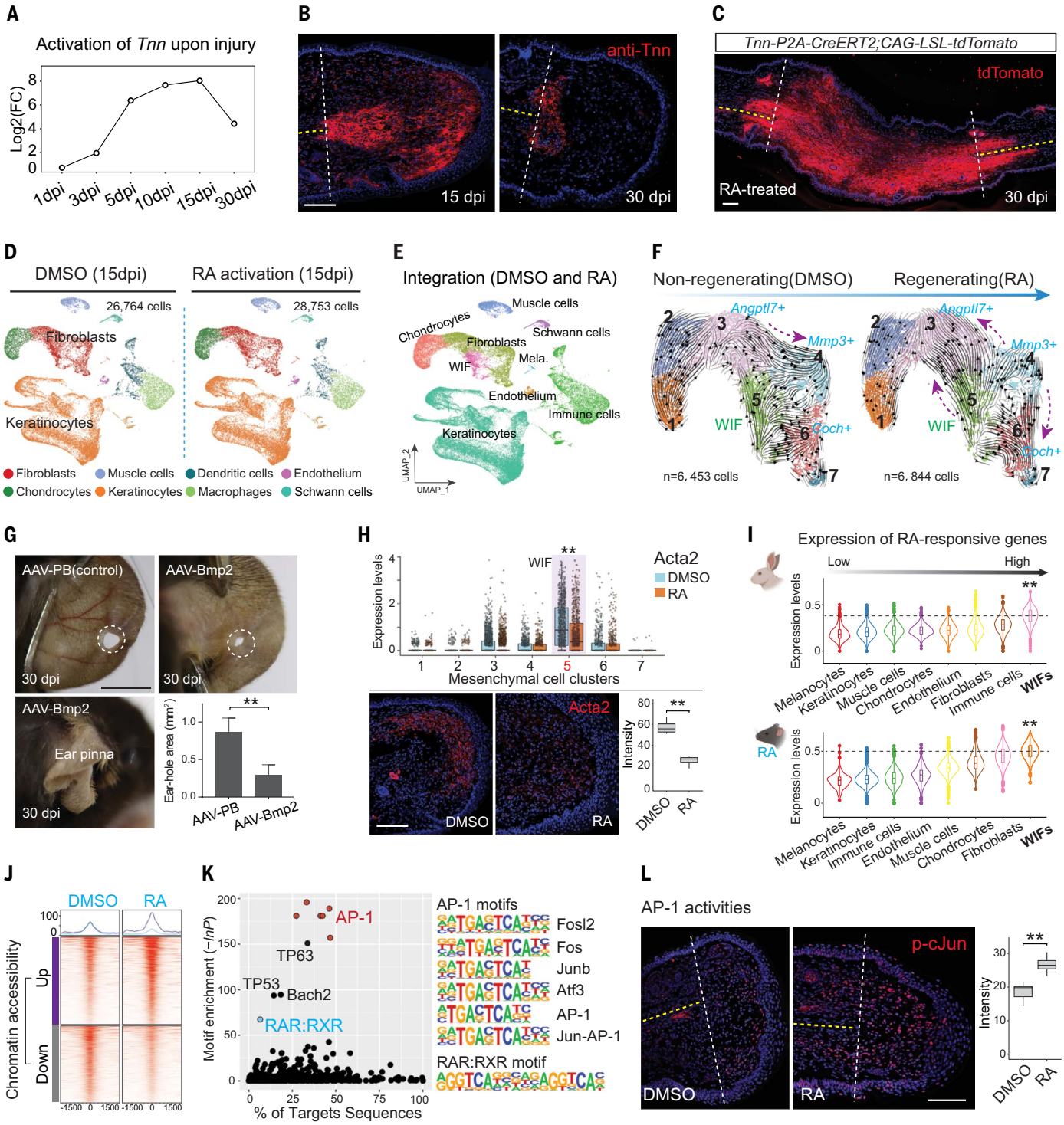

Fig. 5. Reactivation of RA signaling promotes WIF-mediated tissue morphogenesis and AP-1 activities. (**A** and **B**) Dynamic expression of *Tnn* at the RNA (A) and protein (B) levels in mouse ear pinna. (**C**) The regenerated mesenchymal tissues were fully occupied by tdTomato-positive cells in RA- and tamoxifen-treated *Tnn-P2A-CreERT2;CAG-LSL-tdTomato* mice. (**D**) UMAP plot showing the major cell populations identified at 15 dpi in RA-treated and DMSO-treated mice. (**E**) Integration of single cells identified from the DMSO and RA groups. (**F**) The response of mesenchymal cells was altered during RA-induced regeneration compared with the control. The purple arrows highlight the major differences between DMSO and RA groups. (**G**) Activation of *Bmp2* using AAV reduced the ear hole size compared with the control. $n = 5$. $^{**}P < 0.01$ (Student's *t*-test). Scale bar, 4 mm. Activation of *Bmp2* frequently altered the morphology of ear pinna. (**H**) The expression of *Acta2* (α-SMA) was significantly down-regulated upon RA treatment. (Top) scRNA-seq data. $^{**}P < 0.01$ (Wilcoxon tests). (Bottom) Acta2 expression detected by anti-Acta2. $^{**}P < 0.01$ (Student's *t*-test). (**I**) WIFs showed the highest RA response compared with other cell types during ear pinna regeneration. $^{**}P < 0.01$ (Wilcoxon test). (**J**) Heatmap for up- and down-regulated peaks detected by ATAC-seq at 15 dpi in RA-treated mice. (**K**) Motifs enriched in the up-regulated peaks detected by ATAC-seq upon RA treatment. (**L**) Phosphorylation of the cJun protein was significantly increased upon the activation of RA signaling. $^{**}P < 0.01$ (Student's *t*-test). Scale bar, 100 μm.

and RA-treated mice (Fig. 5I). Our data suggest that activation of the RA pathway transformed the nonregenerating response into a rabbit-like response and directed WIFs to form new tissues.

RA signaling promotes the transcriptional activity of the AP-1 complex during regeneration

To understand the genome-wide transcriptional changes upon the reactivation of RA signaling, we collected the tissues at the wounding site during blastema formation at 15 dpi and profiled the chromatin accessibility using assay for transposase-accessible chromatin sequencing (ATAC-seq). Our analyses unveiled 2376 up-regulated and 1592 down-regulated peaks compared with the control (Fig. 5J and table S4). The motif enrichment analysis for these RA-induced peaks identified the Activator protein 1 (AP-1), TP63, TP53, Bach2, and the binding motifs of the nuclear retinoic acid receptors (RXR-RAR) as the most enriched ones (Fig. 5K). The enrichment of RXR-RAR motifs validated the biological effect of RA. The AP-1 complex, a heterodimer composed of Jun, Fos, Maf, and ATF family proteins, is essential for the activation of regeneration-responsive enhancers and regeneration in teleost fish, which possesses remarkable regenerative capacities (*2*, *67*). It has been shown that the DNA-binding capacity and stability of this complex are regulated through post-translational phosphorylation (*68*). A side-by-side comparison between the control and RA-treated animals using the phospho-c-Jun (Ser73) antibody showed that the activation of RA signaling augmented Jun phosphorylation (Fig. 5L). Unlike previously identified negative regulation of AP-1 activation in cancer cell lines (*69*, *70*), our data highlight a function of RA signaling in promoting AP-1 activity during tissue regeneration.

Mice lack regulatory elements responsible for the activation of *Aldh1a2* upon ear pinna injury

The transcriptional activation of gene expression is usually achieved through *cis*-regulatory modules such as enhancers and promoters, which control when and where transcription occurs (*71*, *72*). To determine how the expression of *Aldh1a2* fails to be activated during mice ear pinna injury, we assayed H3K4me3 and H3K27ac enrichment at 0 and 10 dpi in mouse and rabbit genomes to identify active promoters and enhancers, respectively. Our results uncovered 786 injury-induced enhancers that did not overlap with the promoters in mice, whereas this number increased to 2628 in rabbits (fig. S18A). In accord with the expression of *Aldh1a2* in each species (Fig. 4, C and D), we detected significant up-regulation of H3K4me3 and H3K27ac peaks at the rabbit *Aldh1a2* promoter (*Rb-Apr*) region but down-regulation at the mouse *Aldh1a2* promoter (*M-Apr*) region (Fig. 6, A and B). Meanwhile, we identified six active enhancers (*AE1-AE6*), as defined by the H3K27ac peaks, at rabbit *Aldh1a2* locus, with *AE1* and *AE5* being regeneration-responsive (Fig. 6A). By contrast, only one active enhancer was found in mice, with activities mainly detected during homeostasis (Fig. 6B). The Aldh1a2 protein is highly conserved in mammals and this gene locus shares a conserved synteny in rabbits, mice, and rats (fig. S18B and Fig. 6, A and B). A genomic comparison of the rabbit, mouse, and rat *Aldh1a2* locus using the VISTA alignment tool suggested that the orthologous regions of *AE1-AE6* were present in mouse and rat genomes (fig. S18C). However, the regulatory activities of these orthologous regions, except the *AE3*, were lost in mouse ear pinna (Fig. 6B).

Next, we created a high-resolution view of 3D genome organization for rabbit blastema to validate enhancer-dependent *Aldh1a2* regulation using Micro-C (*73*). Our data revealed complex chromatin folding during ear pinna regeneration, including topologically associated domains (TADs) and enhancer-promoter or promoter-promoter interactions (Fig. 6C and fig. S19). For instance, highly nested 3D interactions were captured in a TAD with genes involved in fundamental biological processes including DNA repair (*Nhej1*), protein folding (*Dnajb2*), and secretory vesicles (*Ptprn*) (fig. S19B). Our analysis also identified many additional enhancer-promoter and promoter-promoter interactions for the WIF-associated genes such as *Sfrbp1*, *Sncaip*, *Nes*, *Wnt11*, *Lef1*, and *Wnt5a* (fig. S19, C to G), supporting relatively high quality of the data. Next, we employed the Micro-C, H3K27ac ChIP-seq, and ATAC-seq data to dissect the chromatin interactions at the rabbit *Aldh1a2* locus. The analysis displayed intricate physical chromatin contacts (arrowheads) including promoter-enhancer interactions (*Rb-Apr-AE1* and *Rb-Apr-AE4*) and other interactions with unknown functions (Fig. 6D). Unlike *AE1*, *AE4* also interacted with an undefined open chromatin region (star) in addition to the *Rb-Apr*. We failed to detect direct chromatin contacts between the second regenerative-responsive enhancer *AE5* and the *Rb-Apr*, which implied that *AE5* either did not regulate *Aldh1a2* or interacted weakly with other unknown elements within this locus. Thus, the robust activation of *Aldh1a2* expression upon tissue damage in rabbits was under control of distinct regulatory elements (*Rb-Apr*, *AE1*, *AE4*, and undefined elements), whereas the activities of these elements were barely detected in mice.

A single rabbit enhancer is sufficient to promote ear pinna regeneration in transgenic mice

To validate the activities of the identified promoters and enhancers experimentally, we took *Rb-Apr*, *M-Apr*, and *AE1* as examples to conduct transgenic reporter assays by inserting each reporter cassette into the mouse *Rosa26* locus (fig. S20). Consistent with the H3K4me3 ChIP-seq and RNA-seq data, the expression of green fluorescent protein (GFP) driven by *Rb-Apr* was much stronger than *M-Apr* in homeostatic and injured ear pinna (Fig. 6, E and F, and fig. S20D). Nonetheless, both *Rb-Apr* and *M-Apr* could direct reporter gene expression in the testis, indicating that the diminished regulatory activity in the ear pinna for *M-Apr* was not due to the positional effect of the *Rosa26* locus (fig. S20E). The GFP expression driven by *AE1* was detected in both epithelial cells and mesenchymal cells after tissue damage, with relatively stronger expression in the epidermis (Fig. 6G). Unexpectedly, we observed broad homeostatic enhancer activities of *AE1* in various organs including lungs, brains, kidneys, and intestines (fig. S21A). The multiple alignments of 60 vertebrate species showed that *AE1* contains an ancient regulatory module with sequence conservation across different mammals including the platypus (fig. S21B), indicating the pleiotropic functions and deep evolutionary origin of this enhancer. Among the tested promoters and enhancers, we did not observe a robust blastemal enrichment of GFP expression resembling the endogenous *Aldh1a2* expression in rabbits (Fig. 4C). Our data confirmed the regulatory activities for the identified elements and suggested that the precise *Aldh1a2* expression likely requires the involvement of all regulatory inputs identified in Micro-C.

Because of the sufficiency of RA signaling in rescuing rat ear pinna regeneration and the substantial reduction in *Aldh1a2* expression upon injury (Fig. 4J and Fig. 6H), we asked whether loss of regulatory activities for *Aldh1a2*-linked enhancers also occurred in rats. ATAC-seq was performed to profile open chromatin regions associated with rat ear pinna at 0 and 10 dpi. No injury-activated open chromatin regions were present at 10 dpi compared with intact tissues (Fig. 6H), supporting that the activities of orthologous enhancers responsible for the injury-dependent activation of *Aldh1a2* were absent in rat ear pinna. Next, we hypothesized that if the loss of activities of regulatory elements (promoter and enhancers) is the major mechanism underlying the deficiency of *Aldh1a2* expression upon injury in mice and rats, transgenic animals carrying all rabbit *Aldh1a2*-linked regulatory elements should be able to promote regeneration in these animals. Ideally, transgenic mice with the whole rabbit *Aldh1a2* locus should achieve an accurate spatial-temporal enzyme expression with proper intensity after injury. However, the appropriate 460-kilobase size of the locus makes it challenging to test. Alternatively, we can test the ability of individual elements (promoter or enhancer) to stimulate ear pinna regeneration. Because a single element cannot confer full

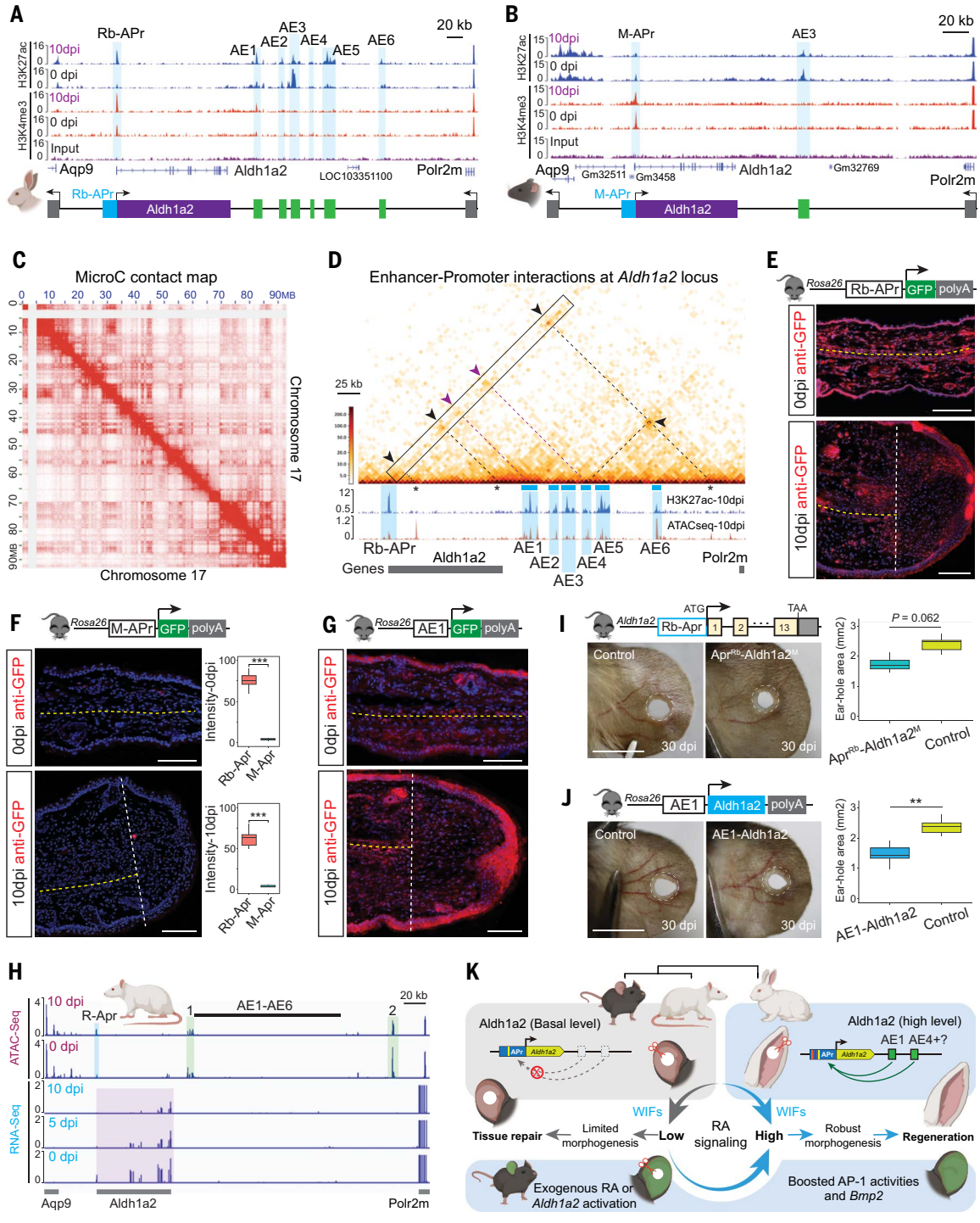

Fig. 6. Evolutionary inactivation of regulatory modules mediated the suppression of *Aldh1a2* in mice. (**A** and **B**) Identification of active enhancers and promoters at the *Aldh1a2* locus in rabbits (A) and mice (B). (**C**) Heatmap showing Micro-C robustly captured the chromatin interactions at 10 dpi in rabbits. The heatmap was plotted using the Micro-C interaction maps (binned at 100 kb resolution) for chromosome 17 where *Aldh1a2* is located. (**D**) Micro-C captured enhancer-promoter interactions at the *Aldh1a2* locus at 10 dpi in rabbits. Arrowheads indicate the chromatin interactions; purple arrowheads mark the contacts between *Rb-Apr* and *AE1/AE4*. Stars highlight the undefined elements that interact with *Rb-Apr*. (**E**) A 4-kb rabbit *Aldh1a2* promoter (*Rb-Apr*) was sufficient to drive GFP expression during homeostasis and injury in transgenic mice. GFP was visualized using an anti-GFP antibody. (**F**) The expression of GFP driven by a 4-kb mouse *Aldh1a2* promoter (*M-Apr*) was barely detectable in transgenic mice. ***$P < 0.001$ (Student's *t*-test). (**G**) The rabbit *AE1* enhancer was sufficient to drive GFP expression during homeostasis and injury in transgenic mice. Scale bar, 100 μm. (**H**) ATAC-seq failed to detect injury-activated open chromatin regions upon rat ear pinna injury. The transcription of *Aldh1a2* was diminished after injury (bottom). 1 and 2, two open chromatin regions present during homeostasis. *R-Apr*, rat *Aldh1a2* promoter. The region that contains the *AE1-AE6* orthologous sequence (black line) is not accessible in rats. (**I**) The Apr^{Rb}-$Aldh1a2^{M}$ (promoter swap) transgenic mice displayed reduced ear hole size at 30 dpi compared with the control. $n = 6$. $P = 0.062$ (Student's *t*-test). (**J**) Forced expression of *Aldh1a2* driven by the rabbit *AE1* enhancer significantly promoted ear pinna regeneration in *AE1-Aldh1a2* mice compared with the control. $n = 6$. **$P < 0.01$ (Student's *t*-test). Scale bar, 4 mm. (**K**) A working model showing the mechanism responsible for the failure of ear pinna regeneration in mice and rats during evolution.

control of the enzyme expression, it is unlikely that we would observe a complete rescue of ear pinna regeneration but some improvement in regeneration should be possible. To test this idea, we generated transgenic mice to swap the endogenous mouse *Aldh1a2* promoter with the rabbit promoter (*Apr^{Rb}-Aldh1a2^{M}*) and to reactivate the expression of *Aldh1a2* after injury using the rabbit *AE1* (*AE1-Aldh1a2*, fig. S20, G to I), respectively. Compared with the control, *Apr^{Rb}-Aldh1a2^{M}* mice seemed to display reduced ear hole size at 30 dpi, although no statistical significance was observed ($P = 0.062$, Fig. 6I). However, the rabbit *AE1* was sufficient to significantly ($P < 0.01$) improve the ear pinna regeneration in *AE1-Aldh1a2* mice (Fig. 6J). The insufficiency of *AE1* alone in fully rescuing regeneration confirms that other elements are also required for the precise control of the spatial-temporal enzyme expression with proper intensity. Consistent with the extent of regeneration, we observed distinct expression levels of *Aldh1a2* in gene-rescue experiments in descending order as *AAV-Aldh1a2*, *AE1-Aldh1a2*, and *Apr^{Rb}-Aldh1a2^{M}* (fig. S21C). Altogether, our data suggest that changes in the *Aldh1a2*-linked regulatory elements contribute to the deficiency of *Aldh1a2* expression upon injury.

Discussion

As a seemingly beneficial trait, regeneration is maintained in some lineages but has been lost in many others during evolution (*1*). By performing comparative studies between regenerative and nonregenerative species, we found that the RA pathway is a direct target involved in the evolution of mouse and rat ear pinna regeneration (Fig. 6K). The deficiency of *Aldh1a2* expression, prompted by the loss of activities of multiple regulatory elements, leads to insufficient production of RA in mice and rats. As a result, these animals form a blastema with an altered microenvironment and limited morphogenesis after injury. Reactivation of RA signaling could partially transform the mouse injury response into a rabbit-like regeneration response and direct WIFs to restore damaged tissues. In addition to the crucial roles in development and diseases (*60*, *74*), RA signaling activities are involved in various contexts of regeneration including bone, limb, skin, nerve, and lung regeneration (*61*, *62*, *75*–*80*). The RA machinery is also found in invertebrates. Indeed, the receptor RXR has an ancient evolutionary origin and is present in genomes of basal metazoans such as cnidarians and sponges (*81*, *82*). The deep conservation and the wide involvement of RA signaling in different stages of regeneration imply that modulation of RA production may be a hot spot for the change of regenerative capacities during evolution.

The RA precursor, vitamin A, cannot be synthesized de novo by animals and must be obtained directly from the diet in the form of carotenoids or retinyl esters. Unlike most physiological functions controlled by its bioactive metabolite RA, animal vision requires the unprocessed vitamin A for visual phototransduction (*74*), which adds an extra layer of regulation for the RA pathway. The activities of diurnal, nocturnal, and crepuscular animals are largely based on the levels of light. For both predators and prey, successful adaptation in a specific environment usually involves the modulation of structures or performance related to hearing and vision, by which tight regulation of the RA pathway is required (*74*, *83*). In terms of the ear pinna, distinct sizes, positions, and orientations have evolved to assist the brain in sensing front, rear, or upper sound sources or to serve additional functions for animals living in special environments (*84*, *85*). For example, the enlarged ear pinnae in rabbits, hares, Townsend's big-eared bats, and the long-eared jerboa provide an efficient way to distinguish between ambient noise and the sounds of predators or prey, and serve as a critical organ for thermoregulation during hot summers or after energetic motions (*86*, *87*). Recent evidence also suggests that the acquisition of endothermy and the metabolic shift from glycolysis to fatty acid oxidation contributed to cardiomyocyte cell-cycle arrest in adult mammals incapable of heart regeneration (*88*–*90*). We propose that the emergence of a distinct organ function for environmental adaptation is the potential driving force for the evolution of regeneration. Our findings may help in increasing understanding of the evolution of regeneration and provide a potential framework for dissecting mechanisms underpinning the failure of regeneration in different organs and species.

Material and methods summary

Detailed materials and methods can be found in the supplementary materials. Briefly, 2-mm and 4-mm full-thickness holes were punched through the ear pinna in small mammals (mice and rats) and relatively larger mammals (rabbits and goats), respectively. Samples for regeneration or tissue repair at specific time points were collected using Biopsy punches with larger diameters (4 mm for mice and rats; 8 mm for rabbits and goats). Bulk RNA-seq was carried out to identify injury-responsive genes. Three biological replicates were prepared for each time point. Six adult mice, rats, and rabbits and five adult goats were used for each biological replicate. Single-cell RNA-seq was conducted to identify cell populations involved in ear pinna regeneration and repair. For WT mice and rabbits, the ear hole tissues were collected at 0, 5, and 10 dpi while tissue from RA-treated and DMSO-treated mice were collected at 15 dpi. The fresh tissues from six adult animals were pooled, cut into small pieces, and subjected to cell dissociation. The libraries were prepared using the 10X Genomics platform. The spatial transcriptomics for rabbit ear pinna regeneration and mouse ear pinna repair were conducted using Stereo-seq. Fresh ear pinna samples from mice and rabbits (0 dpi, 5 dpi, and 10 dpi) were collected, quickly embedded into the optimal cutting temperature compound, and snap-frozen with dry ice. For each sample, 10-μm cryosections were collected onto the Stereo-seq chip. To identify active promoters and enhancers in rabbits and mice upon tissue injury, we carried out H3K4me3 and H3K27ac ChIP-seq, respectively. ATAC-seq was performed in rats to identify injury-activated open chromatin regions.

Six transgenic mouse lines including *Tnn-P2A-CreERT2*, *Rb-Apr-GFP*, *M-Apr-GFP*, *AE1-GFP*, *Apr^{Rb}-Aldh1a2^{M}*, and *AE1-Aldh1a2* were generated in this study. Specifically, the *Tnn-P2A-CreERT2* line was generated by inserting the *P2A-CreERT2* cassette into the final exon of the gene *Tnn* using CRISPR/Cas9-mediated homologous recombination. The *Rb-Apr-GFP*, *M-Apr-GFP*, and *AE1-GFP* transgenic reporter mice were created by knocking in the expression cassette into the *Rosa26* locus. Two transgenic mouse lines used for the rescue experiments, *Apr^{Rb}-Aldh1a2^{M}* and *AE1-Aldh1a2*, were created by swapping the endogenous mouse *Aldh1a2* promoter with the rabbit promoter and by knocking in the *AE1-Aldh1a2* expression cassette into the *Rosa26* locus, respectively.

REFERENCES AND NOTES

1. A. E. Bely, K. G. Nyberg, Evolution of animal regeneration: Re-emergence of a field. *Trends Ecol. Evol.* **25**, 161–170 (2010). doi: 10.1016/j.tree.2009.08.005; pmid: 19800144
2. W. Wang *et al.*, Changes in regeneration-responsive enhancers shape regenerative capacities in vertebrates. *Science* **369**, eaaz3090 (2020). doi: 10.1126/science.aaz3090; pmid: 32883834
3. M. Gemberling, T. J. Bailey, D. R. Hyde, K. D. Poss, The zebrafish as a model for complex tissue regeneration. *Trends Genet.* **29**, 611–620 (2013). doi: 10.1016/j.tig.2013.07.003; pmid: 23927865
4. E. M. Tanaka, P. W. Reddien, The cellular basis for animal regeneration. *Dev. Cell* **21**, 172–185 (2011). doi: 10.1016/j.devcel.2011.06.016; pmid: 21763617
5. T. Hirsch *et al.*, Regeneration of the entire human epidermis using transgenic stem cells. *Nature* **551**, 327–332 (2017). doi: 10.1038/nature24487; pmid: 29144448
6. H. Lin *et al.*, Lens regeneration using endogenous stem cells with gain of visual function. *Nature* **531**, 323–328 (2016). doi: 10.1038/nature17181; pmid: 26958831
7. R. Hayashi *et al.*, Co-ordinated ocular development from human iPS cells and recovery of corneal function. *Nature* **531**, 376–380 (2016). doi: 10.1038/nature17000; pmid: 26958835
8. H. Lorach *et al.*, Walking naturally after spinal cord injury using a brain-spine interface. *Nature* **618**, 126–133 (2023). doi: 10.1038/s41586-023-06094-5; pmid: 37225984
9. K. Wei *et al.*, Epicardial FSTL1 reconstitution regenerates the adult mammalian heart. *Nature* **525**, 479–485 (2015). doi: 10.1038/nature15372; pmid: 26375005

10. M. O. Karl *et al.*, Stimulation of neural regeneration in the mouse retina. *Proc. Natl. Acad. Sci. U.S.A.* **105**, 19508–19513 (2008). doi: 10.1073/pnas.0807453105; pmid: 19033471
11. L. Todd *et al.*, Efficient stimulation of retinal regeneration from Müller glia in adult mice using combinations of proneural bHLH transcription factors. *Cell Rep.* **37**, 109857 (2021). doi: 10.1016/j.celrep.2021.109857; pmid: 34686336
12. N. L. Jorstad *et al.*, Stimulation of functional neuronal regeneration from Müller g lia in adult mice. *Nature* **548**, 103–107 (2017). doi: 10.1038/nature23283; pmid: 28746305
13. T. M. Brushart *et al.*, Electrical stimulation promotes motoneuron regeneration without increasing its speed or conditioning the neuron. *J. Neurosci.* **22**, 6631–6638 (2002). doi: 10.1523/JNEUROSCI.22-15-06631.2002; pmid: 12151542
14. R. O. Becker, Stimulation of partial limb regeneration in rats. *Nature* **235**, 109–111 (1972). doi: 10.1038/235109a0; pmid: 4550399
15. M. Mizell, Limb regeneration: Induction in the newborn opossum. *Science* **161**, 283–286 (1968). doi: 10.1126/science.161.3838.283; pmid: 5657335
16. S. Grade, M. Götz, Neuronal replacement therapy: Previous achievements and challenges ahead. *NPJ Regen. Med.* **2**, 29 (2017). doi: 10.1038/s41536-017-0033-0; pmid: 29302363
17. J. B. Bryson *et al.*, Optical control of muscle function by transplantation of stem cell-derived motor neurons in mice. *Science* **344**, 94–97 (2014). doi: 10.1126/science.1248523; pmid: 24700859
18. T. Martin *et al.*, A Cretaceous eutriconodont and integument evolution in early mammals. *Nature* **526**, 380–384 (2015). doi: 10.1038/nature14905; pmid: 26469049
19. R. J. Goss, The evolution of regeneration: Adaptive or inherent? *J. Theor. Biol.* **159**, 241–260 (1992). doi: 10.1016/S0022-5193(05)80704-0; pmid: 1294847
20. T. R. Gawriluk *et al.*, Comparative analysis of ear-hole closure identifies epimorphic regeneration as a discrete trait in mammals. *Nat. Commun.* **7**, 11164 (2016). doi: 10.1038/ncomms11164; pmid: 27109826
21. P. K. Williams-Boyce, J. C. Daniel Jr., Comparison of ear tissue regeneration in mammals. *J. Anat.* **149**, 55–63 (1986). pmid: 3693110
22. R. J. Goss, Prospects of regeneration in man. *Clin. Orthop. Relat. Res.* **151**, 270–282 (1980). pmid: 7418317
23. P. R. Manger, L. S. Hall, J. D. Pettigrew, The development of the external features of the platypus (Ornithorhynchus anatinus). *Philos. Trans. R. Soc. B* **353**, 1115–1125 (1998). doi: 10.1098/rstb.1998.0270; pmid: 9720109
24. M. A. Vorontsova, L. D. Liozner, *Asexual propagation and regeneration*. (Pergamon Press, 1960), pp. 489 p.
25. A. W. Seifert *et al.*, Skin shedding and tissue regeneration in African spiny mice (Acomys). *Nature* **489**, 561–565 (2012). doi: 10.1038/nature11499; pmid: 23018966
26. B. Riddell *et al.*, Complex tissue regeneration in *Lophuromys* reveals a phylogenetic signal for enhanced regenerative ability in deomyine rodents. *Proc. Natl. Acad. Sci. U.S.A.* **122**, e2420726122 (2025). doi: 10.1073/pnas.2420726122; pmid: 39793030
27. A. W. Seifert, K. Muneoka, The blastema and epimorphic regeneration in mammals. *Dev. Biol.* **433**, 190–199 (2018). doi: 10.1016/j.ydbio.2017.08.007; pmid: 29291973
28. C. M. Brewer *et al.*, Adaptations in Hippo-Yap signaling and myofibroblast fate underlie scar-free ear appendage wound healing in spiny mice. *Dev. Cell* **56**, 2722–2740.e6 (2021). doi: 10.1016/j.devcel.2021.09.008; pmid: 34610329
29. A. Tomasso, T. Koopmans, P. Lijnzaad, K. Bartscherer, A. W. Seifert, An ERK-dependent molecular switch antagonizes fibrosis and promotes regeneration in spiny mice (*Acomys*). *Sci. Adv.* **9**, eadf2331 (2023). doi: 10.1126/sciadv.adf2331; pmid: 37126559
30. P. Sass *et al.*, Epigenetic inhibitor zebularine activates ear pinna wound closure in the mouse. *EBioMedicine* **46**, 317–329 (2019). doi: 10.1016/j.ebiom.2019.07.010; pmid: 31303499
31. J. Liu *et al.*, Regenerative phenotype in mice with a point mutation in transforming growth factor beta type I receptor (TGFBR1). *Proc. Natl. Acad. Sci. U.S.A.* **108**, 14560–14565 (2011). doi: 10.1073/pnas.1111056108; pmid: 21841138
32. P. Sosnowski *et al.*, Regenerative Drug Discovery Using Ear Pinna Punch Wound Model in Mice. *Pharmaceuticals (Basel)* **15**, 610 (2022). doi: 10.3390/ph15050610; pmid: 35631437
33. Y. Zhang *et al.*, Drug-induced regeneration in adult mice. *Sci. Transl. Med.* **7**, 290ra92 (2015). doi: 10.1126/scitranslmed.3010228; pmid: 26041709
34. K. Bedelbaeva *et al.*, Lack of p21 expression links cell cycle control and appendage regeneration in mice. *Proc. Natl. Acad. Sci. U.S.A.* **107**, 5845–5850 (2010). doi: 10.1073/pnas.1000830107; pmid: 20231440
35. K. L. Mack *et al.*, Allele-specific expression reveals genetic drivers of tissue regeneration in mice. *Cell Stem Cell* **30**, 1368–1381.e6 (2023). doi: 10.1016/j.stem.2023.08.010; pmid: 37714154
36. M. A. Nishiguchi, C. A. Spencer, D. H. Leung, T. H. Leung, Aging Suppresses Skin-Derived Circulating SDF1 to Promote Full-Thickness Tissue Regeneration. *Cell Rep.* **24**, 3383–3392.e5 (2018). doi: 10.1016/j.celrep.2018.08.054; pmid: 30257200
37. J. Simkin, T. R. Gawriluk, J. C. Gensel, A. W. Seifert, Macrophages are necessary for epimorphic regeneration in African spiny mice. *eLife* **6**, e24623 (2017). doi: 10.7554/eLife.24623; pmid: 28508748
38. R. F. Abarca-Buis, E. Krötzsch, Proximal ear hole injury heals by limited regeneration during the early postnatal phase in mice. *J. Anat.* **242**, 402–416 (2023). doi: 10.1111/joa.13782; pmid: 36317926
39. Q. S. Zhang, D. S. Kurpad, M. G. Mahoney, M. J. Steinbeck, T. A. Freeman, Inhibition of apoptosis signal-regulating kinase 1 alters the wound epidermis and enhances auricular cartilage regeneration. *PLOS ONE* **12**, e0185803 (2017). doi: 10.1371/journal.pone.0185803; pmid: 29045420
40. J. A. Goldman, K. D. Poss, Gene regulatory programmes of tissue regeneration. *Nat. Rev. Genet.* **21**, 511–525 (2020). doi: 10.1038/s41576-020-0239-7; pmid: 32504079
41. C. L. Stoick-Cooper *et al.*, Distinct Wnt signaling pathways have opposing roles in appendage regeneration. *Development* **134**, 479–489 (2007). doi: 10.1242/dev.001123; pmid: 17185322
42. Q. M. Phan *et al.*, Lef1 expression in fibroblasts maintains developmental potential in adult skin to regenerate wounds. *eLife* **9**, e60066 (2020). doi: 10.7554/eLife.60066; pmid: 32990218
43. K. D. Poss, J. Shen, M. T. Keating, Induction of lef1 during zebrafish fin regeneration. *Dev. Dyn.* **219**, 282–286 (2000). doi: 10.1002/1097-0177(2000)9999:9999<::AID-DVDY1045>3.3.CO;2-3; pmid: 11002347
44. E. Quint *et al.*, Bone patterning is altered in the regenerating zebrafish caudal fin after ectopic expression of sonic hedgehog and bmp2b or exposure to cyclopamine. *Proc. Natl. Acad. Sci. U.S.A.* **99**, 8713–8718 (2002). doi: 10.1073/pnas.122571799; pmid: 12060710
45. Y. Mori *et al.*, Identification of fibroblast growth factor-18 as a molecule to protect adult articular cartilage by gene expression profiling. *J. Biol. Chem.* **289**, 10192–10200 (2014). doi: 10.1074/jbc.M113.524090; pmid: 24577103
46. Y. C. Lin, S. R. Roffler, Y. T. Yan, R. B. Yang, Disruption of Scube2 Impairs Endochondral Bone Formation. *J. Bone Miner. Res.* **30**, 1255–1267 (2015). doi: 10.1002/jbmr.2451; pmid: 25639508
47. G. S. Gulati *et al.*, Single-cell transcriptional diversity is a hallmark of developmental potential. *Science* **367**, 405–411 (2020). doi: 10.1126/science.aax0249; pmid: 31974247
48. D. C. LeBert *et al.*, Matrix metalloproteinase 9 modulates collagen matrices and wound repair. *Development* **142**, 2136–2146 (2015). doi: 10.1242/dev.121160; pmid: 26015541
49. D. J. Behonick *et al.*, Role of matrix metalloproteinase 13 in both endochondral and intramembranous ossification during skeletal regeneration. *PLOS ONE* **2**, e1150 (2007). doi: 10.1371/journal.pone.0001150; pmid: 17987127
50. J. Vukovic *et al.*, Lack of fibulin-3 alters regenerative tissue responses in the primary olfactory pathway. *Matrix biology* **28**, 406–415 (2009). doi: 10.1371/journal.pone.0001150; pmid: 17987127
51. L. Eklund *et al.*, Lack of type XV collagen causes a skeletal myopathy and cardiovascular defects in mice. *Proc. Natl. Acad. Sci. U.S.A.* **98**, 1194–1199 (2001). doi: 10.1073/pnas.98.3.1194; pmid: 11158616
52. R. Browaeys, W. Saelens, Y. Saeys, NicheNet: Modeling intercellular communication by linking ligands to target genes. *Nat. Methods* **17**, 159–162 (2020). doi: 10.1038/s41592-019-0667-5; pmid: 31819264
53. S. Kahai, S. C. Lee, A. Seth, B. B. Yang, Nephronectin promotes osteoblast differentiation via the epidermal growth factor-like repeats. *FEBS Lett.* **584**, 233–238 (2010). doi: 10.1016/j.febslet.2009.11.077; pmid: 19944102
54. A. Bailón-Plaza, A. O. Lee, E. C. Veson, C. E. Farnum, M. C. van der Meulen, BMP-5 deficiency alters chondrocytic activity in the mouse proximal tibial growth plate. *Bone* **24**, 211–216 (1999). doi: 10.1016/S8756-3282(98)00171-9; pmid: 10071913
55. S. E. Iismaa *et al.*, Comparative regenerative mechanisms across different mammalian tissues. *NPJ Regen. Med.* **3**, 6 (2018). doi: 10.1038/s41536-018-0044-5; pmid: 29507774
56. H. Li *et al.*, Dynamic cell transition and immune response landscapes of axolotl limb regeneration revealed by single-cell analysis. *Protein Cell* **12**, 57–66 (2021). doi: 10.1007/s13238-020-00763-1; pmid: 32748350
57. B. Munz *et al.*, Overexpression of activin A in the skin of transgenic mice reveals new activities of activin in epidermal morphogenesis, dermal fibrosis and wound repair. *EMBO J.* **18**, 5205–5215 (1999). doi: 10.1093/emboj/18.19.5205; pmid: 10508154
58. D. Gay *et al.*, Fgf9 from dermal γδ T cells induces hair follicle neogenesis after wounding. *Nat. Med.* **19**, 916–923 (2013). doi: 10.1038/nm.3181; pmid: 23727932
59. N. B. Ghyselinck, G. Duester, Retinoic acid signaling pathways. *Development* **146**, dev167502 (2019). doi: 10.1242/dev.167502; pmid: 31273085
60. T. J. Cunningham, G. Duester, Mechanisms of retinoic acid signalling and its roles in organ and limb development. *Nat. Rev. Mol. Cell Biol.* **16**, 110–123 (2015). doi: 10.1038/nrm3932; pmid: 25560970
61. S. P. Allen, M. Maden, J. S. Price, A role for retinoic acid in regulating the regeneration of deer antlers. *Dev. Biol.* **251**, 409–423 (2002). doi: 10.1006/dbio.2002.0816; pmid: 12435367
62. N. Blum, G. Begemann, Retinoic acid signaling controls the formation, proliferation and survival of the blastema during adult zebrafish fin regeneration. *Development* **139**, 107–116 (2012). doi: 10.1242/dev.065391; pmid: 22096078
63. N. Blum, G. Begemann, Retinoic acid signaling spatially restricts osteoblasts and controls ray-interray organization during zebrafish fin regeneration. *Development* **142**, 2888–2893 (2015). doi: 10.1242/dev.120212; pmid: 26253402

64. M. T. Tierney *et al.*, Vitamin A resolves lineage plasticity to orchestrate stem cell lineage choices. *Science* **383**, eadi7342 (2024). doi: 10.1126/science.adi7342; pmid: 38452090
65. F. Le Doze, D. Debruyne, F. Albessard, L. Barre, G. L. Defer, Pharmacokinetics of all-trans retinoic acid, 13-cis retinoic acid, and fenretinide in plasma and brain of Rat. *Drug Metab. Dispos.* **28**, 205–208 (2000). doi: 10.1016/S0090-9556(24)15129-X; pmid: 10640519
66. S. D. Ahadome *et al.*, Classical dendritic cells mediate fibrosis directly via the retinoic acid pathway in severe eye allergy. *JCI Insight* **1**, e87012 (2016). doi: 10.1172/jci.insight.87012; pmid: 27595139
67. X. Jia, W. Lin, W. Wang, Regulation of chromatin organization during animal regeneration. *Cell Regen. (Lond.)* **12**, 19 (2023). doi: 10.1186/s13619-023-00162-x; pmid: 37259007
68. R. J. Davis, Signal transduction by the JNK group of MAP kinases. *Cell* **103**, 239–252 (2000). doi: 10.1016/S0092-8674(00)00116-1; pmid: 11057897
69. X. F. Zhou, X. Q. Shen, L. Shemshedini, Ligand-activated retinoic acid receptor inhibits AP-1 transactivation by disrupting c-Jun/c-Fos dimerization. *Mol. Endocrinol.* **13**, 276–285 (1999). doi: 10.1210/mend.13.2.0237; pmid: 9973257
70. C. Caelles, J. M. González-Sancho, A. Muñoz, Nuclear hormone receptor antagonism with AP-1 by inhibition of the JNK pathway. *Genes Dev.* **11**, 3351–3364 (1997). doi: 10.1101/gad.11.24.3351; pmid: 9407028
71. R. Andersson, A. Sandelin, Determinants of enhancer and promoter activities of regulatory elements. *Nat. Rev. Genet.* **21**, 71–87 (2020). doi: 10.1038/s41576-019-0173-8; pmid: 31605096
72. R. C. Hardison, J. Taylor, Genomic approaches towards finding cis-regulatory modules in animals. *Nat. Rev. Genet.* **13**, 469–483 (2012). doi: 10.1038/nrg3242; pmid: 22705667
73. T. H. Hsieh *et al.*, Mapping Nucleosome Resolution Chromosome Folding in Yeast by Micro-C. *Cell* **162**, 108–119 (2015). doi: 10.1016/j.cell.2015.05.048; pmid: 26119342
74. K. Niederreither, P. Dollé, Retinoic acid in development: Towards an integrated view. *Nat. Rev. Genet.* **9**, 541–553 (2008). doi: 10.1038/nrg2340; pmid: 18542081
75. S. R. Scadding, M. Maden, Retinoic acid gradients during limb regeneration. *Dev. Biol.* **162**, 608–617 (1994). doi: 10.1006/dbio.1994.1114; pmid: 8150219
76. D. Correa-Gallegos *et al.*, CD201^{+} fascia progenitors choreograph injury repair. *Nature* **623**, 792–802 (2023). doi: 10.1038/s41586-023-06725-x; pmid: 37968392
77. S. Sinha *et al.*, Fibroblast inflammatory priming determines regenerative versus fibrotic skin repair in reindeer. *Cell* **185**, 4717–4736.e25 (2022). doi: 10.1016/j.cell.2022.11.004; pmid: 36493752
78. M. Maden, Retinoic acid in the development, regeneration and maintenance of the nervous system. *Nat. Rev. Neurosci.* **8**, 755–765 (2007). doi: 10.1038/nrn2212; pmid: 17882253
79. M. Hind, M. Maden, Retinoic acid induces alveolar regeneration in the adult mouse lung. *Eur. Respir. J.* **23**, 20–27 (2004). doi: 10.1183/09031936.03.00119103; pmid: 14738226
80. R. Ferreira, J. Napoli, T. Enver, L. Bernardino, L. Ferreira, Advances and challenges in retinoid delivery systems in regenerative and therapeutic medicine. *Nat. Commun.* **11**, 4265 (2020). doi: 10.1038/s41467-020-18042-2; pmid: 32848154
81. H. K. Biesalski *et al.*, Modulation of myb gene expression in sponges by retinoic acid. *Oncogene* **7**, 1765–1774 (1992). pmid: 1323819
82. Z. Kostrouch *et al.*, Retinoic acid X receptor in the diploblast, Tripedalia cystophora. *Proc. Natl. Acad. Sci. U.S.A.* **95**, 13442–13447 (1998). doi: 10.1073/pnas.95.23.13442; pmid: 9811819
83. A. Cvekl, W. L. Wang, Retinoic acid signaling in mammalian eye development. *Exp. Eye Res.* **89**, 280–291 (2009). doi: 10.1016/j.exer.2009.04.012; pmid: 19427305
84. G. A. Manley, Comparative Auditory Neuroscience: Understanding the Evolution and Function of Ears. *J. Assoc. Res. Otolaryngol.* **18**, 1–24 (2017). doi: 10.1007/s10162-016-0579-3; pmid: 27539715
85. A. Le Maître, N. D. S. Grunstra, C. Pfaff, P. Mitteroecker, Evolution of the Mammalian Ear: An Evolvability Hypothesis. *Evol. Biol.* **47**, 187–192 (2020). doi: 10.1007/s11692-020-09502-0; pmid: 32801400
86. R. W. Hill, J. H. Veghte, Jackrabbit ears: Surface temperatures and vascular responses. *Science* **194**, 436–438 (1976). doi: 10.1126/science.982027; pmid: 982027
87. R. Araújo *et al.*, Inner ear biomechanics reveals a Late Triassic origin for mammalian endothermy. *Nature* **607**, 726–731 (2022). doi: 10.1038/s41586-022-04963-z; pmid: 35859179
88. K. Hirose *et al.*, Evidence for hormonal control of heart regenerative capacity during endothermy acquisition. *Science* **364**, 184–188 (2019). doi: 10.1126/science.aar2038; pmid: 30846611
89. A. C. Cardoso *et al.*, Mitochondrial Substrate Utilization Regulates Cardiomyocyte Cell Cycle Progression. *Nat. Metab.* **2**, 167–178 (2020). doi: 10.1038/s42255-020-0169-x; pmid: 32617517
90. X. Li *et al.*, Inhibition of fatty acid oxidation enables heart regeneration in adult mice. *Nature* **622**, 619–626 (2023). doi: 10.1038/s41586-023-06585-5; pmid: 37758950
91. W. Lin, X. Jia, X. Shi, Code for Omics data analysis regarding ear pinna regeneration. Zenodo, (2025); https://doi.org/10.5281/zenodo.15272641.

ACKNOWLEDGMENTS

We thank A. S. Alvarado, S. Morrison, P. Newmark, J. Xiong, C.-K. Hu, I. Harel, K. Chen, Y. Yu, and B. Shen for helpful discussion and suggestions on the manuscript; we also thank all members of the Wang lab for comments. We thank Q. Li from NIBS genetic screening center for AAV packaging and purification, D. Chen for advice on cell dissociation, S. Zang for help on rabbit and goat sample collection, and Y. Yin for help with scRNA-seq library preparation. We thank the NIBS Animal and Plant center, Imaging center, and the Molecular Biology and Cytometry facility for their help, and the Beijing Laboratory Animal Research Center for maintaining the rabbits and rats. **Funding:** W.W. is supported by the National Key R&D Program of China (2023YFA1800600) and by the National Institute of Biological Sciences, Beijing. **Author contributions:** W.F.L., X.H.J., and W.W. conceived the project and designed the experiments. W.F.L., X.H.J., L.P.Z., M.Q.W., Y.F.L., T.F.R., Y.Y.L., and S.Q.L. performed the experiments. Q.Y.H. completed the goat regeneration experiments under the supervision of J.L. X.F.S., P.Y.Z., H.H.D., S.Y.H., J.M.K., X.C., H.X.S., and Z.Q.D. from BGI Research performed Stereo-seq and Stereo-seq–related data analysis. W.F.L., X.L.Z., and W.W. performed computational data analysis. All authors contributed to the interpretation of the results. W.F.L. and W.W. wrote the manuscript. All authors reviewed the manuscript. **Competing interests:** W.W., W.F.L., X.H.J., M.Q.W., and Y.Y.L. have filed a Chinese patent application (application no. 202410504588.8) on the use of a combination of retinoic acid and its degradation inhibitor in promoting tissue regeneration. All other authors declare no competing interests. **Data and materials availability:** Sequencing data have been deposited to the Sequence Read Archive (SRA) under BioProject PRJNA1055264. The spatial transcriptome data of this study have been deposited into STOmis DB of China National GeneBank DataBase (CNGBdb) with accession number STT0000077. All mouse lines created in this study will be made available upon request. All code is deposited at Zenodo (*91*).

SUPPLEMENTARY MATERIALS

science.org/doi/10.1126/science.adp0176
Materials and Methods; Figs. S1 to S21; Tables S1 to S4; References (*92*–*97*); MDAR Reproducibility Checklist

Submitted 4 March 2024; resubmitted 26 January 2025; accepted 24 April 2025
10.1126/science.adp0176